

Self-replication of a pulse in excitable reaction-diffusion systems

Yumino Hayase

Department of Physics, Graduate School of Sciences, Kyushu University, Fukuoka 812-8581, Japan

Takao Ohta

Institute for Nonlinear Sciences and Applied Mathematics, Graduate School of Sciences, Hiroshima University, Higashi-Hiroshima 739-8526, Japan

(Received 16 April 2002; published 24 September 2002)

We investigate self-replication of a pulse in Bonhoeffer–van der Pol type reaction-diffusion systems in one dimension. The interface dynamics of front and back of a pulse developed for a bistable system is extended to a monostable case, which is useful to clarify the mechanism of the self-replication. We shall show that the threshold parameter for excitability plays the central role for self-replication. The present theory can be applied not only to a symmetric pulse, but also to a propagating asymmetric pulse.

DOI: 10.1103/PhysRevE.66.036218

PACS number(s): 05.45.–a, 82.20.–w

I. INTRODUCTION

Self-replication of a pulse in reaction-diffusion media has been observed in real experiments and in numerical simulations since the early 90s. In the ferrocyanide-iodate-sulfate chemical reaction, domains having a high p H concentration grow and beyond a critical size, each of them deform and splits into two domains [1]. A quite similar phenomenon has been obtained by numerical simulations of the Gray-Scott model in two dimensions [2]. In one-dimensional simulations, self-replication of a pulse has been found not only in the Gray-Scott model [3] but also in other excitable reaction diffusion systems, such as the Bonhoeffer–van der Pol (BvP) model [4] and the Prague model [5,6]. Therefore, the self-replication is very common to excitable media. Furthermore, it has been found that self-replication causes regular self-similar spatiotemporal patterns [4,7,8].

At present, there are a few theoretical studies of these self-replications. A qualitative analysis of the transient behavior of an unstable pulse near a saddle-node bifurcation has been made [9]. A more quantitative theory including self-replication of a traveling pulse has been proposed by Ei *et al.* to focus on the slow manifold associated with the pulse motion [10]. However, self-replication of a breathing pulse has not been studied so far.

In the present paper, we investigate the condition for self-replication of a pulse in excitable reaction-diffusion systems in one dimension. First, we consider a breathing pulse where the pulse width is oscillating. In the singular limit, such that the interfaces (front and back) of a pulse is much smaller than the pulse width, we derive the equation of motion for the interacting interfaces, which is applicable not only to a bistable situation but also to a monostable situation. The theory starts with the assumption that there is a pair of interfaces for a single pulse. However, we will show that this assumption does not always hold when the system is excitable and this is an indication of self-replication. Next, we generalize the theory for self-replication of a propagating pulse. Although our analysis does not provide a rigorous criterion for self-replication, it will be useful to see qualitatively the reason as to why self-replication occurs for certain

parameter regime and its initial value dependence.

In Sec. II, we summarize the behavior of self-replication of a pulse obtained numerically in several reaction-diffusion systems. The interface dynamics for a breathing pulse in the Bonhoeffer–van der Pol type reaction-diffusion equation is given in Sec. III, and the condition for self-replication is derived. In Sec. IV, we extend our analysis to self-replication of a propagating pulse. Discussion of the results obtained is given in Sec. V.

II. VARIOUS TYPES OF SELF-REPLICATION

In this section, we summarize the properties of self-replication of a pulse found in reaction-diffusion systems, which is classified as follows.

(1) By changing the parameters, a motionless pulse becomes unstable in an excitable reaction-diffusion system when the pulse width exceeds a certain critical value and splits symmetrically into two pulses. This has been studied by Kerner and Osipov [11]. A similar replication is also found in the Gray-Scott model given by Eqs. (4) and (5) given below [12].

(2) A breathing pulse self-replicates at the instant that its width becomes maximum [8]. Figure 1(a) shows an example obtained in the BvP-type equations,

$$\tau \frac{\partial u}{\partial t} = D_u \frac{\partial^2 u}{\partial x^2} + f(u) - v, \quad (1)$$

$$\frac{\partial v}{\partial t} = D_v \frac{\partial^2 v}{\partial x^2} + u - \gamma v, \quad (2)$$

where

$$f(u) = bu(u - a_1)(1 - u). \quad (3)$$

The parameters in Fig. 1(a) are chosen as $D_u = 0.09$, $D_v = 1$, $a_1 = 0$, $b = 10$, $\gamma = 0.38$, and $\tau = 0.37$. To our knowledge, this type of self-replication has not been reported previously.

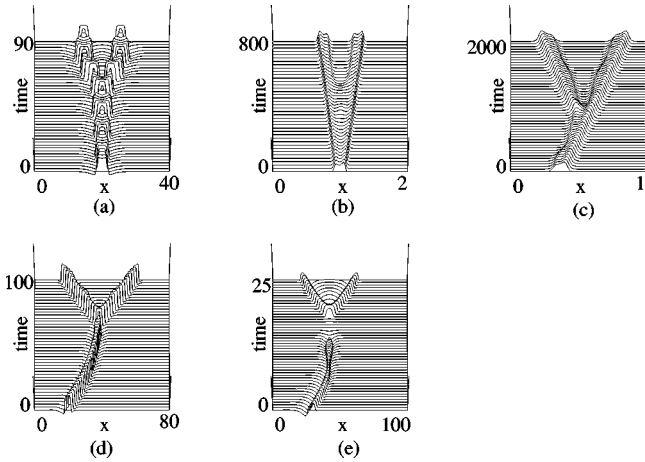


FIG. 1. (a) Self-replication of a breathing pulse in the BvP model, Eqs. (1) and (2) with Eq. (3). The parameters are $D_u = 0.09$, $D_v = 1$, $a_1 = 0$, $b = 10$, $\gamma = 0.38$, and $\tau = 0.37$. (b) Self-replication of a pulse in Gray-Scott model, Eqs. (4) and (5). The parameters are $F = 0.04$, $k = 0.0605$, $D_u = 2.0 \times 10^{-5}$, and $D_v = 1.0 \times 10^{-5}$. (c) Self-replication of a traveling pulse in Gray-Scott model, Eqs. (4) and (5). The parameters are $F = 0.025$ and $k = 0.0551$. Other parameters are the same as in (b). (d) Self-replication of a traveling pulse in the BvP model, Eqs. (1) and (2) with Eq. (3). The parameters are the same as in (a) except for $\tau = 0.3$. (e) Self-replication of a traveling pulse in the BvP model with hyperbolic nonlinearity, Eqs. (1) and (2) with Eq. (6). The parameters are $D_u = 1$, $D_v = 10$, $\tau = 0.35$, $a_2 = 0.1$, $\delta = 0.05$, and $\gamma = 0$. All the quantities in this figure and Figs. 2–10 below are dimensionless.

(3) A pulse increases its width monotonically and splits into two pulses [8]. An example is displayed in Fig. 1(b) for the Gray-Scott model,

$$\frac{\partial u}{\partial t} = D_u \frac{\partial^2 u}{\partial x^2} - uv^2 + F(1 - u), \quad (4)$$

$$\frac{\partial v}{\partial t} = D_v \frac{\partial^2 v}{\partial x^2} + uv^2 - (F + k)v. \quad (5)$$

The parameters used in Fig. 1(b) are $F = 0.04$, $k = 0.0605$, $D_u = 2.0 \times 10^{-5}$, and $D_v = 1.0 \times 10^{-5}$.

(4) A propagating pulse produces a daughter pulse at the tail region. This has been found in the Gray-Scott model [3,9] and an exothermic reaction-diffusion model [13]. The case of the Gray-Scott model is shown in Fig. 1(c) where the parameters are $F = 0.025$, $k = 0.0551$, $D_u = 2.0 \times 10^{-5}$, and $D_v = 1.0 \times 10^{-5}$. A similar splitting of a pulse has also been obtained in the Prague model [8].

(5) A propagating pulse splits into two pulses not at the tail region but at the middle of a pulse. This occurs in the set of Eqs. (1) and (2) with Eq. (3) for the parameters, for example, $\tau = 0.3$. Other parameters are the same as those in Fig. 1(a). This type of self-replication is shown in Fig. 1(d).

(6) A pulse becomes very small and then survives again splitting into two pulses, which is found in the BvP model (1) and (2) with a hyperbolic tangent nonlinearity [4,7]

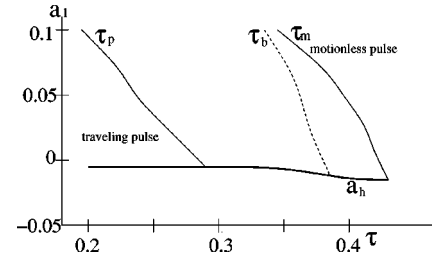


FIG. 2. Phase diagram in the a_1 - τ plane in the BvP model, Eqs. (1) and (2) with Eq. (3). The BvP model has a subcritical Hopf bifurcation point $a_1 = a_h$ such that a limit cycle solution appears when $a_1 < a_h$. For $\tau < \tau_p$, a traveling pulse is stable, whereas a motionless pulse is stable for $\tau > \tau_m$. A breathing motion appears in the interval $\tau_b < \tau < \tau_m$.

$$f(u) = \frac{1}{2} \left[\tanh \frac{u - a_2}{\delta} + \tanh \frac{a_2}{\delta} \right] - u, \quad (6)$$

where a_2 and δ are positive constants. An example is shown in Fig. 1(e) where $a_2 = 0.1$, $\gamma = 0$, $\delta = 0.05$, $\tau = 0.35$, $D_u = 10$, and $D_v = 1$.

All of these results have been obtained by computer simulations. So far, only a few theoretical investigations have been made. As mentioned in the Introduction, we shall propose a criterion for self-replication, which is useful to understand the mechanism of self-replications shown above and their mutual relationship.

III. INTERFACE DYNAMICS FOR A BREATHING PULSE

The Bonhoeffer-van der Pol system (1) and (2) with the cubic nonlinearity (3) reveals a variety of pulse dynamics. Figure 2 represents a phase diagram obtained numerically.

By choosing the parameters in which the system is monostable, a traveling pulse exists for $\tau < \tau_p$, where τ_p is a certain bifurcation threshold. There is another bifurcation point $\tau_m (> \tau_p)$ such that when $\tau < \tau_m$, a motionless pulse undergoes a breathing oscillation. This breathing pulse becomes unstable for $\tau < \tau_b (< \tau_m)$. Therefore, there is a parameter regime $\tau_p < \tau < \tau_b$ where only a uniform solution is stable. It is emphasized, however, that remarkable pulse dynamics is found in this apparently trivial region. When the parameter a_1 is decreased keeping the monostability of the system, one can obtain a self-replicating pulse in this region $\tau_p < \tau < \tau_b$ [7]. For $\tau \lesssim \tau_b$, a breathing pulse self-replicates as in Fig. 1(a), whereas for $\tau \gtrsim \tau_p$, a self-replicating traveling pulse appears as in Fig. 1(d).

To analyze the self-replication in a tractable way, we modify slightly Eqs. (1) and (2),

$$\tau \epsilon \frac{\partial u}{\partial t} = \epsilon^2 \frac{\partial^2 u}{\partial x^2} + f(u) - v, \quad (7)$$

$$\frac{\partial v}{\partial t} = D \frac{\partial^2 v}{\partial x^2} + u - \gamma v, \quad (8)$$

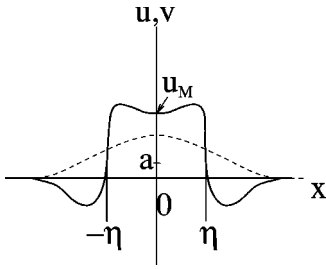


FIG. 3. The spatial variation of u (solid line) and v (broken line) for a symmetric pulse.

where we have replaced τ in Eq. (1) by $\epsilon\tau$ and D_u by ϵ^2 . In the limit $\epsilon^2 \ll D$ as we assume, the set of Eqs. (7) and (8) is a prototype of excitable systems.

For a technical convenience, we employ a simplified piecewise linear form for $f(u)$,

$$f(u) = -u + \theta(u - a), \quad (9)$$

where $\theta(x) = 1$ for $x > 0$ and $\theta(x) = 0$ for $x < 0$. This form of $f(u)$ is obtained from Eq. (6) by taking the limit $\delta \rightarrow 0$.

In this section, we consider a symmetric pulse of Eqs. (7) and (8) with Eq. (9), as shown in Fig. 3. In the limit $\epsilon^2 \ll D$, the motion of a pulse can be represented in terms of the position of the interfaces $x = \pm \eta(t)$, which is defined through the relation

$$u(\pm \eta(t), t) = a. \quad (10)$$

When $\gamma > a/(1-a)$, the set of Eqs. (7) and (8) with Eq. (9) has two linearly stable uniform equilibrium solutions. That is, the system is bistable. In this situation, the equation of motion for the interface has been derived by the singular-perturbation method [14]. See also Ref. [15]. Here we do not go into the details, but describe only the essential steps of the derivation.

At the interface, the spatial variation of u is very steep whereas that of v is quite smooth. Therefore, in the length scale of the interface width, one may replace v in Eq. (7) by the value at the interface v_I . As a result, the interface equation of motion is given for a fixed value of v_I by

$$\frac{\tau \dot{\eta}}{\sqrt{(\tau \dot{\eta})^2 + 4}} = 1 - 2a - 2v_I. \quad (11)$$

The value of v_I is evaluated by solving Eq. (8). In the limit $\epsilon \rightarrow 0$, we obtain from Eq. (7),

$$u = \theta(\eta - x)\theta(\eta + x) - v. \quad (12)$$

Substituting this into Eq. (8) and applying the short-time expansion that is valid as far as the interface velocity is small enough [14], we obtain $v(x, t)$ and hence $v_I = v(\pm \eta, t)$. By using the condition of the location of an interface (10), the final form of the interface equation of motion is given by

$$m \ddot{\eta} = 1 - 2a - \frac{1}{\beta \phi} [\phi - \dot{\eta} - (\phi + \dot{\eta}) \exp(-2\eta/\ell)] - \frac{\tau \dot{\eta}}{\sqrt{(\tau \dot{\eta})^2 + 4}}, \quad (13)$$

where

$$\phi = (\dot{\eta}^2 + 4D\beta)^{1/2}, \quad (14)$$

$$\ell = \frac{2D}{\phi - \dot{\eta}}, \quad (15)$$

$$m = \frac{3}{8\beta^{5/2}\sqrt{D}} \left[1 + \exp(-2\kappa\eta) + \left[\frac{3\eta}{4\beta^2 D} + \frac{\eta^2}{2D^{3/2}\beta^{3/2}} \right] \times \exp(-2\kappa\eta) \right], \quad (16)$$

with $\beta = 1 + \gamma$ and $\kappa = (\beta/D)^{1/2}$.

By analyzing Eq. (13), one notes that there is a stable motionless pulse when $1 - 2a - 1/\beta < 0$ and $\tau > \tau_B$, where the threshold value τ_B generally depends on a and β . On the other hand, when $\tau < \tau_B$, a motionless pulse turns out unstable and undergoes a breathing oscillation.

IV. SELF-REPLICATION OF A BREATHING PULSE

It should be noted that we have not used the condition that the system is bistable in the derivation of the interface equation of motion (13). Therefore, as long as the interface width is much smaller than that of the pulse width, i.e., $\epsilon \ll \eta$, the equation of motion (13) for a pair of interacting interfaces can be applied even for the monostable case that satisfies

$$1 - a < \frac{1}{\beta}. \quad (17)$$

However the derivation of Eq. (13) contains implicitly the assumption that $u > a$ for $-\eta < x < \eta$. If this condition is violated, it means that there exist extra interfaces that contradicts with the presumption that we are dealing with a single pulse. Recall that the interface position has been defined by Eq. (10). Therefore if u inside the pulse becomes smaller than a during the breathing oscillation, this is an indication of self-replication of the pulse.

The variable u must take its minimum value at the center of gravity $x = 0$ for a symmetric pulse. From Eq. (12), we note the relation

$$u = 1 - v \quad (18)$$

for $-\eta < x < \eta$. Therefore after solving Eq. (8), the value $u_M = u(0, t)$ is readily evaluated as

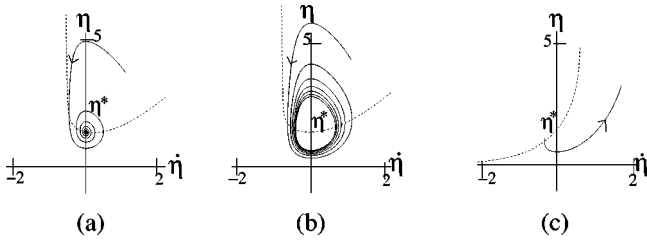


FIG. 4. Trajectory of the solution of the interface equation (13) for (a) $\tau=1.3$, (b) $\tau=1.2$, and (c) $\tau=0.7$. Other parameters are set to be $a=0.05$, $\gamma=0.03$, and $D=1$. The broken line is a line where the right-hand side of Eq. (13) vanishes. η^* is the equilibrium solution.

$$u_M = 1 - \frac{1}{\beta} + \frac{2\ell}{\phi} \exp(-\eta/\ell) - \ddot{\eta} \left[\frac{3}{8\beta^{5/2}D^{1/2}} + \frac{3\eta}{8\beta^2D} + \frac{\eta^2}{8\beta^{3/2}D^{3/2}} \right] \exp(-\kappa\eta). \quad (19)$$

The steady state value is given by

$$u_M^{(eq)} = 1 - \frac{1}{\beta} + \frac{1}{\beta} \exp\left(-\sqrt{\frac{\beta}{D}}\eta\right). \quad (20)$$

This is a decreasing function of η and $u_M^{(eq)} = 1 - 1/\beta$ for $\eta \rightarrow \infty$. This clearly shows that $u_M^{(eq)}$ is smaller than a in the monostable situation given by Eq. (17). Therefore $u_M^{(eq)}$ becomes smaller than a at a certain finite value of η .

As was mentioned at the end of the preceding section, when $\tau > \tau_B$ and

$$\alpha = 1 - 2a - 1/\beta < 0, \quad (21)$$

Equation (13) has a stable motionless pulse solution,

$$\eta^{(eq)} = -\frac{1}{2} \sqrt{\frac{D}{\beta}} \ln(1 + 2a\beta - \beta). \quad (22)$$

In this case, $u_M^{(eq)}$ is given by

$$u_M^{(eq)} = 1 - \frac{1}{\beta} + \frac{1}{\beta} (1 + 2a\beta - \beta)^{1/2}, \quad (23)$$

which is always larger than a .

Now we investigate self-replication of a pulse, which is described by Eqs. (13) and (19). The numerical simulations of Eqs. (1) and (2) with Eq. (3) have revealed that self-replication of a pulse occurs when the equilibrium pulse width is not small in the monostable region. From Eqs. (17), (21), and (22), this is satisfied for $a \sim 0$ and $\beta \sim 1$. In what follows, we analyze Eq. (13) in this condition.

Figure 4 displays the trajectories in the $\eta - \dot{\eta}$ plain for $a=0.05$, $\gamma=0.03$, and $D=1$, and by changing the parameter τ . For these parameters, the bifurcation threshold τ_B is given by $\tau_B=1.22$. In fact, when $\tau=1.3$, the trajectory converges to the equilibrium solution (22), as in Fig. 4(a). For a slightly smaller value of $\tau=1.2$ in Fig. 4(b), a limit cycle oscillation

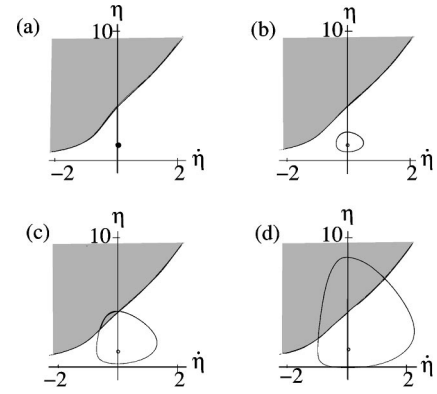


FIG. 5. (a) Equilibrium solution of Eq. (13) for $\tau=1.3$ and limit cycle solution of Eq. (13) for (b) $\tau=1.2$ (c) $\tau=1.17$, and (d) $\tau=1.14$. Other parameter are the same as in Fig. 4. The white dot in (b), (c), and (d) indicates the unstable equilibrium solution. The value of u_M becomes smaller than a in the gray region.

appears corresponding to the breathing motion of the pulse. When $\tau=0.7$, the pulse width η diverges, as in Fig. 4(c). These results are the same as those for the bistable case.

Now we study the situation where self-replication occurs. The regions where the conditions $u_M > a$ and $\eta > 0$ are violated are indicated by the shaded area in Fig. 5. When $\tau=1.3$ in Fig. 5(a), there is a stable equilibrium solution as in Fig. 4(a). When $\tau=1.2$, a breathing oscillation occurs in Fig. 5(b) where the trajectory does not enter the shaded region. However when $\tau=1.17$, the amplitude of the oscillation becomes large as in Fig. 5(c) and the trajectory enters into the region where $u_M > a$. This is an indication of self-replication. If one decreases the value of τ further, both the conditions $u_M < a$ and $\eta < 0$ are not satisfied, as in Fig. 5(d), where $\tau=1.14$. In this case an oscillating pulse undergoes either self-replication or annihilation depending on the initial condition.

Figure 6 displays the time evolution of η and u_M for the same values as in Figs. 5(a), 5(b), and 5(c). In Figs. 6(a) and 6(b), the lowest value of u_M is always larger than a whereas, in Fig. 6(c), u_M becomes smaller than a after several oscillations as indicated by the arrow. This causes a self-replication of the breathing pulse. The reason why the condition $\alpha \leq 0$ is necessary is due to the fact that the unstable equilibrium value $\eta^{(eq)}$ is large in this situation as is seen from Eqs. (21) and (22) so that the trajectory of the limit cycle oscillation easily enters in the region $u_M > a$ before η becomes negative. The time dependence of η and u_M for smaller values of τ is given in Fig. 7 where all other parameters are the same as those in Fig. 5(d). In Fig. 7(a), u_M becomes smaller than a after two times of oscillation at the instant indicated by the arrow in the lower figure. However, starting with the different initial condition, η becomes negative without oscillation at the time indicated by the arrow as in the upper Fig. 7(b) and hence an annihilation of pulse occurs in this case. Koga and Kuramoto [16] have shown that an annihilation of a breathing pulse appears in the manner mentioned above for the values of τ sufficiently below the bifurcation threshold. However, they have not discussed the possibility of self-replication.

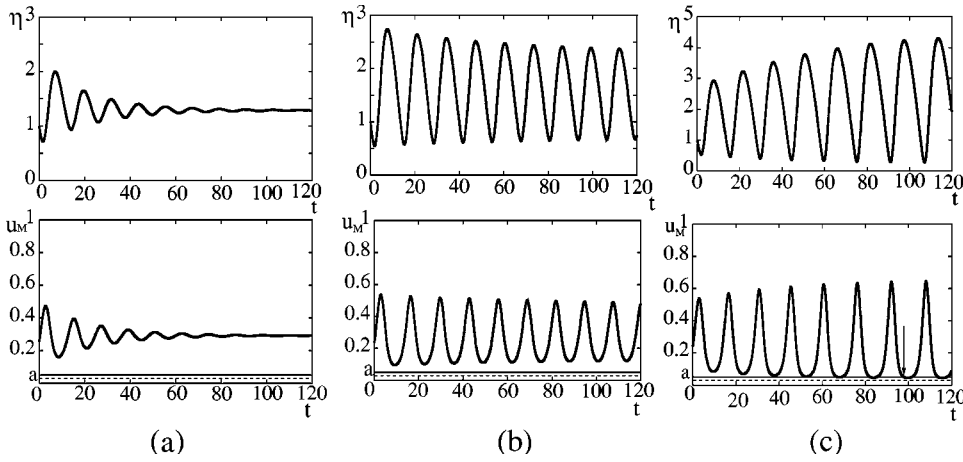


FIG. 6. Time evolution of η and u_M in Eqs. (13) and (19) for (a) $\tau=1.3$, (b) $\tau=1.2$, and (c) $\tau=1.17$. Other parameters are the same as in Fig. 4. The thin line in the lower figures shows the value of a . The vertical arrow in (c) indicates the instant that u_M becomes smaller than a .

When the value of τ is decreased further, the pulse width becomes infinite asymptotically without oscillation. However, the transient behavior of the pulse depends sensitively on the initial condition. Figure 8 displays the typical three cases for $\tau=0.7$. In Fig. 8(a), we start with the initial condition $\dot{\eta}>0$. The middle value u_M decreases and becomes smaller than a at the time indicated by the arrow. This apparently corresponds to the self-replication shown in Fig. 1(b). However, we note the following fact. The interface equation of motion (13) has been derived under the condition that $D_u \ll D_v$, whereas this ratio is of the order of unity in the Gray-Scott model. Therefore, the above similarity should be regarded only as qualitative.

If $\dot{\eta}<0$ initially, η becomes negative before it begins to increase, this implies an annihilation of a pulse. However, if the magnitude of the initial velocity $\dot{\eta}$ (<0) is slightly smaller, one encounters a different situation. The width of the pulse decreases at the early stage. After an elasticlike collision of the two interfaces of the pulse, the pulse begins to expand and then undergoes self-replication as shown in Fig. 8(c).

V. SELF-REPLICATION FOR AN ASYMMETRIC PULSE

Self-replication can be seen not only for a breathing pulse but also for a traveling pulse. Furthermore, in order to re-

present dynamics of a pair of pulses born by self-replication, one needs to formulate self-replication of a transiently traveling pulse.

Dynamics of a traveling pulse can also be described by the interface dynamics for the front z_1 and the back z_2 of a pulse in Fig. 9. Equation of motion for the positions z_1 and z_2 has been derived from Eqs. (7) and (8) with Eq. (9) as [17]

$$m_0 \ddot{z}_1 - n(z_1 - z_2) \ddot{z}_2 = 1 - 2a - 2 \left[\frac{1}{\beta} - c_1 - c_2 \exp[-\kappa_2^{(-)}(z_1 - z_2)] \right] - \frac{\tau \dot{z}_1}{\sqrt{(\tau \dot{z}_1)^2 + 4}}, \quad (24)$$

$$n_0 \ddot{z}_2 - m(z_1 - z_2) \ddot{z}_1 = -1 + 2a + 2 \left[\frac{1}{\beta} - c_1 \exp[-\kappa_1^{(+)}(z_1 - z_2)] - c_2 \right] - \frac{\tau \dot{z}_2}{\sqrt{(\tau \dot{z}_2)^2 + 4}}, \quad (25)$$

where

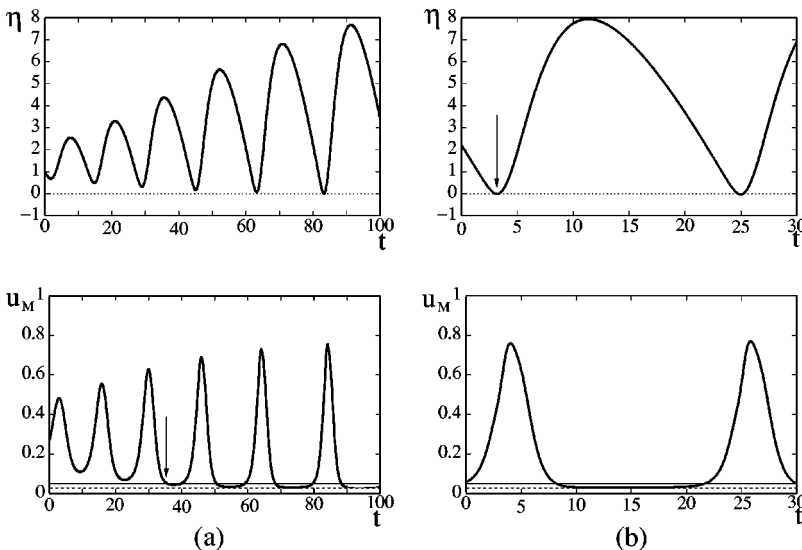


FIG. 7. Time evolution of η and u_M in Eqs. (13) and (19) for $\tau=1.14$. Whether a pulse self-replicates or disappears depends on the initial conditions. The thin line in the lower figures shows the value of a . The arrow in (a) shows the instant where u_M becomes smaller than a whereas the arrow in (b) indicates the time beyond which η becomes negative. Other parameters are the same as in Fig. 4. Initial conditions are different between (a) and (b).

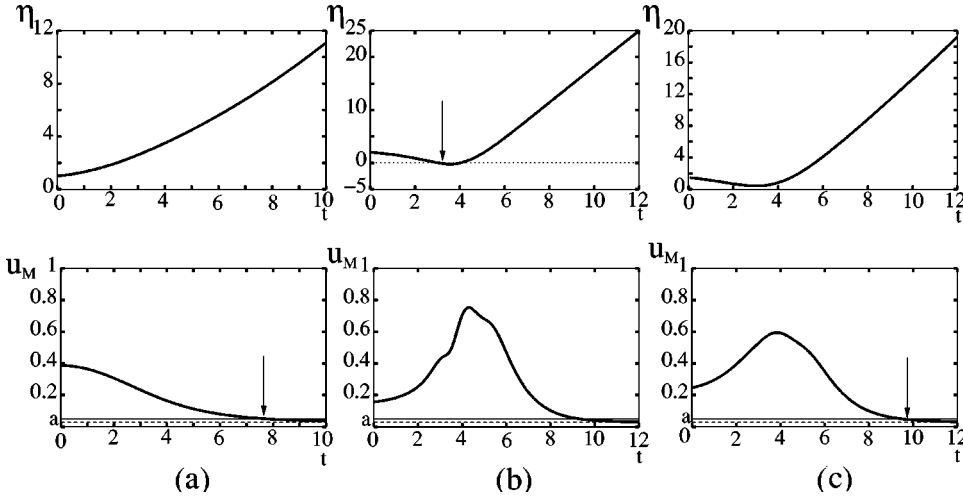


FIG. 8. Time evolution of η and u_M in Eqs. (13) and (19) for $\tau=0.7$, starting with the different initial conditions. The thin line in the lower figures shows the value of a . (a) Monotonous increase of the pulse width causes self-replication at the instant indicated by the arrow beyond which $u_M < a$. (b) A pulse shrinks and disappears at the instant shown by the arrow where η becomes negative. (c) The pulse width decreases first, then increases, and it undergoes self-replication at the instant indicated by the arrow where u_M becomes smaller than a . All the parameters are the same as in Fig. 4(c).

$$m(z) = \left[\frac{12D^2}{\phi_1^5} + \frac{6D}{\phi_1^4}z + \frac{z^2}{\phi_1^3} \right] \exp(-\kappa_1^{(+)}z), \quad (26)$$

$$n(z) = \left[\frac{12D^2}{\phi_2^5} + \frac{6D}{\phi_2^4}z + \frac{z^2}{\phi_2^3} \right] \exp(-\kappa_2^{(-)}z), \quad (27)$$

$$\kappa_i^{(\pm)} = \frac{1}{2D} (\phi_i \mp \dot{z}_i), \quad (28)$$

for $z > 0$ with $\phi_i = (\dot{z}_i^2 + 4\beta D)^{1/2}$ and $m_0 = m(0)$ and $n_0 = n(0)$. This set of equations has been obtained by assuming that the system is bistable. However, by imposing the restriction $u_M > a$ as in the preceding section, Eqs. (24) and (25) can be applied to the monostable case as well.

Since the shape of a traveling pulse is asymmetric with respect to the center of gravity, one needs to determine the position where u takes the minimum value. From the profile of v obtained from Eq. (8) with (12) by the singular perturbation, we have

$$x^* = \frac{1}{(\kappa_1^{(+)} + \kappa_2^{(-)})} \left(\kappa_1^{(+)}z_1 + \kappa_2^{(-)}z_2 + \ln \frac{\phi_1 \kappa_2^{(+)} \kappa_2^{(-)}}{\phi_2 \kappa_1^{(+)} \kappa_1^{(-)}} \right). \quad (29)$$

The value u_M at $x = x^*$ is given by

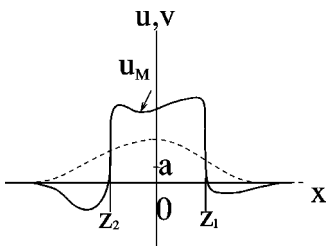


FIG. 9. The spatial variation of u (solid line) and v (broken line) for an asymmetric pulse.

$$u_M = 1 - v_{max} = 1 - \frac{1}{\beta} + \frac{D\kappa_1^{(+)}}{\beta\phi_1} \exp[-\kappa_1^{(+)}(z_1 - x^*)] + \frac{D\kappa_2^{(+)}}{\beta\phi_2} \exp[-\kappa_2^{(-)}(x^* - z_2)]. \quad (30)$$

We solve numerically Eqs. (24), (25), and (30) for the fixed parameters $a = 0.05$, $\gamma = 0.03$, and $D = 1$, as in the preceding section, to study self-replication of a traveling pulse. It is found numerically that a stable traveling pulse appears for $\tau < \tau_p (= 0.78)$.

Since we have removed the symmetry of a pulse and allowed an independent motion for the front and the back, new types of self-replication are possible. One is shown in Fig. 10(a) for $\tau = 0.79$ where a traveling pulse slows down and after an elasticlike collision of the front and the back, the pulse self-replicates. This type of behavior has been observed in the BvP model (1) and (2) with Eq. (3) as in Fig. 1(d).

For a slightly larger value of $\tau = 0.9$, and by choosing the initial condition appropriately, a traveling pulse causes an oscillation of its width once and then undergoes self-replication, as shown in Fig. 10(b). This has been observed in the BvP model in Fig. 6(b) of Ref. [8].

VI. DISCUSSION

So far, no theory has been available to represent quantitatively the process of self-replication. Only the stability of a traveling or a motionless pulse has been formulated mathematically. However, it has not been applied to a breathing pulse.

In the present paper, we have shown that the condition that if the value of u becomes smaller than a inside a pulse, this is an indication of self-replication. Although this is only a necessary condition for self-replication, this criterion is useful for understanding the self-replication of a breathing pulse and a transiently traveling pulse. In fact, our prediction

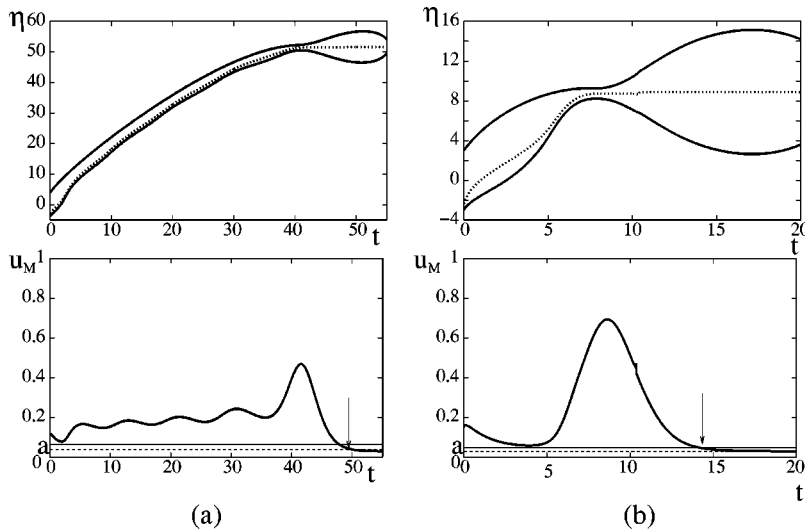


FIG. 10. Time evolution of η and u_M in Eqs. (24), (25), and (30) for (a) $\tau=0.79$ and (b) $\tau=0.9$. The dotted line in the upper figures is the trajectory of the minimum of u in the pulse profile. The thin line in the lower figures shows the value of a . Other parameter are the same as in Fig. 4.

can be compared successfully to those found by computer simulations of several reaction-diffusion equations. The essence of self-replication is the existence of an unstable pulse that does not simply annihilate, but splits into two pulses when the width becomes large. It is noted that the repeated self-replication can also be described by applying successively the methods in Secs. IV and V.

Since self-replication occurs, in two or higher dimensions, through a peanutlike deformation of a domain, the present theory cannot be applied. However, if one combines the stability of a disk-shaped domain and the present criterion u_M

$< a$, it is possible to explore, even in higher dimensions, self-replication of domain which takes an annulus transiently. We hope to return to these problems somewhere in the future.

ACKNOWLEDGMENTS

We would like to thank S. Ei and M. Nagayama for valuable discussions. This work was supported by the Grant-in-Aid of Ministry of Education, Science and Culture of Japan.

-
- [1] K. J. Lee, W. D. McCormick, Q. Ouyang, and H. L. Swinney, *Nature (London)* **369**, 215 (1994).
 - [2] J. E. Pearson, *Science* **261**, 189 (1993).
 - [3] V. Petrov, K. Scott, and K. Showalter, *Philos. Trans. R. Soc. London Ser. A* **347**, 631 (1994).
 - [4] Y. Hayase, *J. Phys. Soc. Jpn.* **66**, 2584 (1997).
 - [5] J. Kosek and M. Marek, *Phys. Rev. Lett.* **74**, 2134 (1995).
 - [6] P. Kastanek, J. Kosek, D. Snita, I. Schreiber, and M. Marek, *Physica D* **84**, 79 (1995).
 - [7] Y. Hayase and T. Ohta, *Phys. Rev. Lett.* **81**, 1726 (1998).
 - [8] Y. Hayase and T. Ohta, *Phys. Rev. E* **62**, 5998 (2000).
 - [9] Y. Nishiura and D. Ueyama, *Physica D* **130**, 73 (1999).
 - [10] S. Ei *et al.*, in *Proceedings of the International Conference on Frontier of Applied Analysis*, 2001 (unpublished).
 - [11] B. S. Kerner and V. V. Osipov, *Autosoliton* (Kluwer, Dordrecht, The Netherlands, 1994).
 - [12] D. Ueyama, *Hokkaido Math.* **28**, 175 (1999).
 - [13] M. Mimura and M. Nagayama, *Chaos* **7**, 817 (1997).
 - [14] T. Ohta, J. Kiyose, and M. Mimura, *J. Phys. Soc. Jpn.* **66**, 1551 (1997).
 - [15] T. Ohta, *Physica D* **151**, 61 (2001).
 - [16] S. Koga and Y. Kuramoto, *Prog. Theor. Phys.* **63**, 105 (1980).
 - [17] M. Mimura, M. Nagayama, H. Ikeda, and T. Ikeda, *Hiroshima Math. J.* **30**, 221 (2000).